ECC
Eurasian Chemical Communications
Original Research Article
http://echemcom.com

Effect of TBAB and SDS surfactants on the interfacial tension of CO_2 Hydrate in water

Hamid Sarlak, Alireza Azimi*, Seyed Mostafa Tabatabaee Ghomshe, Masoomeh Mirzaei

Department of Chemical engineering Mahshahr Branch, Islamic Azad University, Mahshahr, Iran

Received: 15 September 2019, Accepted: 18 November 2019, Published: 02 December 2019

Abstract

The interfacial tension rate is an important factor in the kinetic study of gas hydrate formation. In this study, the interfacial tension between CO_2 hydrate and water was calculated at various temperatures, pressures and solution concentrations through measuring the induction time according to the Classical Nucleation Theory (CNT). Since the nucleation of hydrate is in part an interfacial phenomenon, interfacial properties such as the interfacial tension between gas and water may have a great influence upon the hydrate formation rate. Experimental data for pure water showed that, at constant temperature, with increasing pressure, the interfacial tension decreases from 2.92 to 1.67 mN/m, and at constant pressure with increasing temperature, interfacial tension increases from 3.92 to 4.7 mN/m. At constant temperature, with increasing TBAB concentration from 1% to 3% by weight, the induction time decreases from 60 to 36 seconds. At higher temperatures, addition of SDS 500 ppm decreased the induction time and interfacial tension from 4.61 to 2.32 m N/m. Finally, the relationship of nucleation intensity with the super saturation was obtained by fitting the experimental data. According to equations and graphs, the nucleation intensity is a function of temperature.

Keywords: Classical nucleation theory; interfacial tension; hydrate; super saturation.

Introduction

Capture of CO_2 by hydrate is one of the attractive technologies for reducing greenhouse effect [1]. Gas hydrates, or Clathrate hydrates, which are composed of water molecules and guest (small) molecules like methane, carbon dioxide, etc. guest molecules are encapsulated in the cavities formed by water molecules which are connecting together by hydrogen bonding and gas hydrates are formed [2-6]. Since the nucleation of hydrate is in part an interfacial phenomenon, interfacial properties such as the interfacial tension between gas and water may have a great influence upon the hydrate formation rate [7-13]. Some surfactants are used to slow or prevent hydrate formation in oilfields. On the other hand, some surfactants are used to

*Corresponding author: Alireza Azimi
Tel: +98(911)2150439, Fax: +98(615)2372694
E-mail: aireza_azimi550@yahoo.com

promote hydrate formation in most hydrate-based technologies [14-16]. In this work the interfacial tension between carbon dioxide hydrate and water in presence of SDS and TBAB has been determined through measuring the induction time in carbon dioxide hydrate crystallization. Induction time of crystallization depends on the temperature and the level of super saturation. What follows are related studies on the topic addressed by the current inquiry.

Babaei et al. (2017) investigated the kinetics of semi-Clathrate hydrate formation for the system of argon, tetra N-butyl ammonium bromide (TBAB) and sodium dodecyl sulfate (SDS). The results showed that the induction time decreased with an increase in the initial pressure significantly, and the rate of hydrate formation and moles of Ar consumed increased. With an increase in the TBAB concentration from 0.1 mass fraction to 0.3 mass fraction, the rate of semi-Clathrate hydrate nucleation and formation, and moles of Ar consumed increased, and the induction time decreased significantly. The results also indicated that SDS at concentrations of 100, 200, 400 ppm increased the induction time for semi-Clathrate hydrate formation for the system of Ar + TBAB + water [17].

Azimi et al. (2015) calculated the interfacial tension of methane hydrate through measuring the induction time of methane hydrate crystallization. Experimental results showed a reduction in induction time at constant temperature with increasing super saturation. In addition, the interfacial tension between methane hydrate and the solution was measured at three different temperatures (273.15, 273.65, and 274.65 K). The interfacial tension increased with an increase in the temperature, but it showed no significant change by changing super saturation. A correlation was also used to calculate the order of nucleation [18].

Li et al. (2017) investigated carbon dioxide hydrate formation using a gas-inducing agitated reactor. The results showed that the induction time was greatly shortened from 261 to 24 min as the rotation speed increased from 0 to 800 rpm. In addition, temperature and initial pressure also left strong effects on CO_2 hydrate formation and storage capacity. With a rise in the temperature, the molar mass of dissolved CO_2 increased from 0.18 to 0.25 mol. The storage capacity increased from 0.18 to 0.25mol with increasing pressure. Hence, the gas-inducing agitated reactor can be popularized to improve the hydrate formation efficiency and even be applied to gas storage [19].

Manteghian et al. (2011) determined the interfacial tension between CO_2 hydrate and water at various temperatures, pressures and solution concentrations. The results showed that the induction time decreased with increasing solution concentration at any constant temperature. However, the interfacial tension increased with rising temperature, while changes in super saturation had little effect [20].

Theory

The nucleation rate for a supersaturated solution is calculated by assuming the Classical Nucleation Theory according to the following equation [18,21].

$$\boldsymbol{B = B^0 exp(-\frac{\Delta G}{KT})} \quad (1)$$

The change in Gibbs free energy between a small particle of the dissolved substance and the solute in solution is the sum of the surface free energy and the volume free energy in accordance with Eqs. (2) And (3) [19,22].

$$\boldsymbol{\Delta G_s = 4\pi r^2 \gamma} \quad (2)$$

$$\boldsymbol{\Delta G_v = \frac{4}{3}\pi r^3 g_v} \quad (3)$$

Given the maximum Gibbs free energy in the critical nucleus size and the Gibbs-Thomson equation, the nucleation rate equation will be as follows [18,21].

$$B = B^0 exp(-\frac{16\Pi\gamma^3 v_m^2}{3(kT)(Ln\,S)^2}) \quad (4)$$

Where S is the super saturation, k the Stefan- Boltzmann constant (k=1.3805×10^{-23} j/K), T the temperature, and ν_m is the molecular volume which is obtained from the following equation:

$$S = \frac{C_{eq}}{C^*} \quad (5)$$

$$C_{eq} = \frac{\Delta n}{0.1} \quad (6)$$

$$v_m = \frac{ZRT}{P} \times \frac{1}{N_a} \quad (7)$$

Determination of the interfacial tension

The induction time is proportional to the inverse nucleation.

$$t_{ind} \alpha \frac{1}{B} \quad (8)$$

So:

$$t_{ind} = K\, exp[\frac{16\Pi\gamma^3 v_m^2}{3(kT)^3(Ln\,S)^2}] \quad (9)$$

By taking the natural logarithm of both sides, the equation changes to:

$$Ln(t_{ind}) = Ln\,K + \frac{16\Pi\gamma^3 v_m^2}{3k^3} \times \frac{1}{T^3 Ln\,S^2} \quad (10)$$

Plotting of $Ln(t_{ind})$ versus $\frac{1}{T^3 Ln\,S^2}$ at different temperatures results in a line with the slope m:

$$m = \frac{16\Pi\gamma^3 v_m^2}{3k^3} \quad (11)$$

$$\gamma^3 = K^3 \frac{3m}{16\Pi v_m^2} \quad (12)$$

Taking the third root of Equation (12), the interfacial tension can be obtained in accordance with Equation (13):

$$\gamma = K(\frac{3m}{16\Pi v_m^2})^{\frac{1}{3}} \quad (13)$$

Equations (14) and (15) can be used to compare the interfacial tension obtained from experimental results and those obtained from other equations.

Calculation the order of nucleation

The nucleation rate and the super saturation are related by the following correlation [20]:

$$B = K_b S^n \quad (14)$$

$$t_{ind} = KS^{-n} \quad (15)$$

Taking logarithm of both sides of the above equation, we have:

$$Ln\,t_{ind} = Ln\,K - n\,Ln\,S \quad (16)$$

Method and experiment

Material

Carbon dioxide gas used in the experiments was purchased from the Arvand Industrial Company of gases and had a purity of 99.99%. A 50 lit Capsule CO_2 with an initial pressure of 42 MPa was used in experiments. To analyze hydrate formation, tetra N-butyl ammonium bromide (TBAB) with the chemical formula $NC_{16}H_{36}Br$ was added to the desired solutions as another additive. SDS (Merck Co.) with the chemical formula $NaC_{12}H_{25}SO_4$ was added to the system as a solvent with certain concentrations to analyze hydrate formation. Solutions were prepared using demineralized (DM) Water.

Apparatus

The experiments were performed using a stainless-steel jacketed reactor (SS-316) with an internal volume of 296 cm^3 and a pressure endurance of 200 bars. The internal vessel was equipped with four valves with a pressure endurance of 6000 psi, of which two were ball valves used to inject the solution and drain the water/gas mixture the test, and two were needle valves, one of which was used for gas injection, and the other for connecting to the gas chromatograph and gas sampling. Two openings were provided in the reactor outer wall for the inlet and outlet of the coolant which controlled the reactor temperature through circulation of the refrigerant fluid that was an aqueous solution

containing 50 wt% ethylene glycol. To reduce the energy loss, the hydrate formation reactor and all connections and refrigerant fluid transmission pipes were well insulated. A platinum temperature sensor (Pt-100) with a precision of ±0.1 K was used to measure the reactor internal temperature. The tank pressure was measured with a BD sensor with a precision of about 0.01 MPa. A swing mixer was utilized for to proper mixing in the hydrate formation main tank, and a pump was applied to create vacuum inside the cell. The hydrate formation apparatus used in this study is schematically shown in Figure 1.

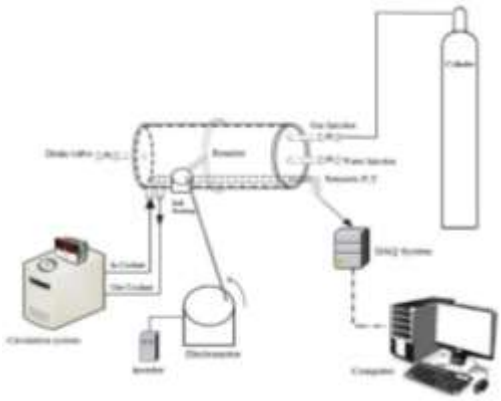

Figure 1. Schematic view of the hydrate formation apparatus

Results and discussion

The general hydrate formation diagram showing the amount of gas consumed over time during hydrate formation is depicted in Figure 2.

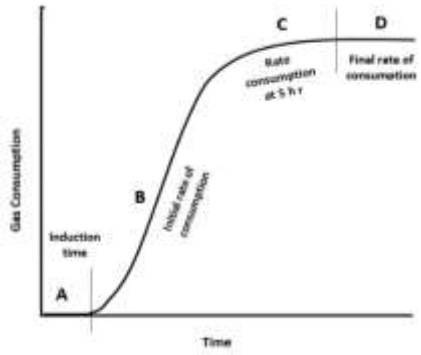

Figure 2. Gas consumption vs. time during hydrate formation

The rate of gas consumption is actually the same as that of the hydrate formation, and the gas consumption is zero at the induction time. Temperature and pressure are constant in the hydrate formation batch system. As seen in Figure 2, Region A shows the induction time while Regions B and C respectively represent the nucleation and growth stages associated with gas consumption [2,23,24].

Hydrate nucleation is an interfacial phenomenon. Therefore, interfacial properties such as interfacial tension between hydrate and water significantly affect hydrate formation [25-27].

In this study, the interfacial tension between water and carbon dioxide hydrate was determined through measuring the induction time. In addition, the order of nucleation and storage capacity of CO_2 gas were calculated.

This paper investigated the effect of different parameters such as the super saturation and temperature on induction time and the effect of temperature and pressure as well as the concentration of the kinetic additive TBAB in the presence of SDS on interfacial tension and order of nucleation.

Super saturation effect

According to literature on the saturation concentration of CO_2 hydrate in water, the induction time decreases with increasing the super saturation [18,19]. To compare the experimental induction times and those calculated from the classical nucleation theory, $\boldsymbol{Ln(t_{ind})}$ was plotted versus $\frac{\mathbf{1}}{\boldsymbol{(Ln\,S)^2}}$ at the constant temperatures of (274.15, 276.15 and 278.15), various pressures and with a constant concentration of the TBAB 1%wt. The induction times for the constant temperatures of 274.15, 276.15, and 278.15 K and three pressures of 36,

38, and 40 bar at TBAB 1%wt are listed in Table 1.

Table 1. Induction times and super saturation data at the initial temperatures and pressures of the experiments

Run	T(K)	P(bar)	t_{ind}	Ln(t_{ind})	1/Ln(s)^2
1	274.15	36	48	3.8712001011	0.458349749
2	274.15	38	90	4.49980967	0.341908081
3	274.15	40	60	4.094344562	0.64234011
4	276.15	36	60	4.094344562	0.414813751
5	276.15	38	60	4.094344562	0.390435863
6	276.15	40	87	4.465908119	0.472884897
7	278.15	36	55	4.007333185	0.395390821
8	278.15	38	54	3.988984047	0.453963407
9	278.15	40	42	3.737669618	0.351289518

As seen in Figures 3 to 5, at the temperatures of 274.15, 276.15, and 278.15 K shows a linear behavior at the constant pressure of 38 bar respectively with a regression coefficient (R^2) of 0.9824, 0.9857, and 0.9793.

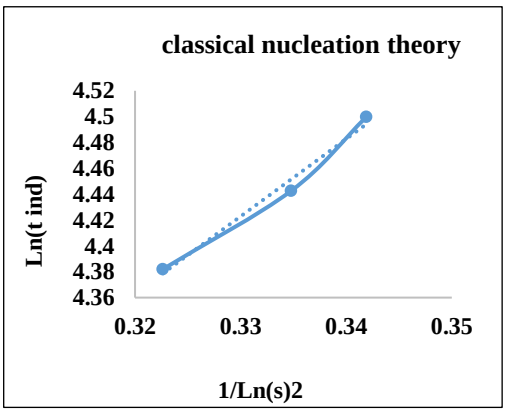

Figure 3. Experimentally determined $\boldsymbol{Ln\ t_{ind}}$ against $\frac{1}{(Ln\ S)^2}$ at 274.15 K and 38 bar

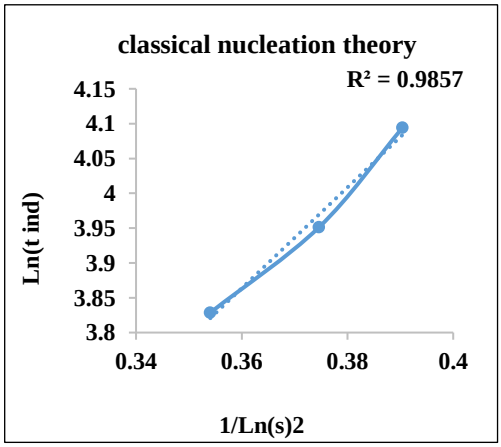

Figure 4. Experimentally determined $\boldsymbol{Ln\ t_{ind}}$ against $\frac{1}{(Ln\ S)^2}$ at 276.15 K and 38 bar

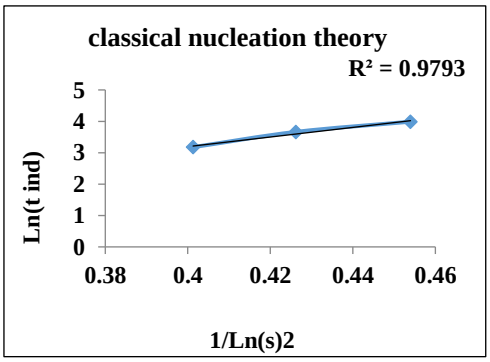

Figure 5. Experimentally determined $\boldsymbol{Ln\ t_{ind}}$ against $\frac{1}{(Ln\ S)^2}$ at 278.15 K and 38 bar

Determination of the interfacial tension

According to Equation 10 and classical nucleation theory at different temperatures, a linear relationship exists between $\boldsymbol{Ln\ t_{ind}}$ and $\frac{1}{Q} = \frac{1}{T^3(Ln\ S)^2}$ with slope $\boldsymbol{m = \frac{16\Pi\gamma^3 v_m^2}{3k^3}}$ (Equation 11) is established so that in Figures 6 through 8, in different thermodynamic conditions, we can observe how interfacial tension changes. The amount of interfacial tension $\boldsymbol{\gamma = K(\frac{3m}{16\Pi v_m^2})^{\frac{1}{3}}}$ in the pressures, temperatures and different concentrations of TBAB and SDS is calculated from the slope of m (Equation 11) and is shown in Tables 2 to 4.

The following equations have been used in the literature to calculate the interfacial tension.

$$\gamma_1 = 0.414KT(C_S N_A)^{\frac{2}{3}} Ln(\frac{C_S}{C^*}) \quad (17)$$

$$\gamma_2 = KTv_m^{-\frac{2}{3}}(0.25)(0.7 - Ln\, x^*) \quad (18)$$

In equations above, used for calculating the interfacial tension, C_S is the molar concentration of hydrate, x* is the mole fraction of solvent, and N_A is the Avogadro number [28-30].

In Table 2, the empirical values of interfacial tension of carbon dioxide were given at different pressures and concentrations of TBAB and SDS additives at a constant temperature of 276 K [31-34].

Table 2. Interfacial tension of CO_2 hydrate at 276 K and different pressures and concentrations of TBAB and SDS as estimated by applying experimental results into the CNT and values calculated using Eqs. (17) and (18)

P(bar)	TBAB (%wt)	SDS(gr)	$\gamma_{exp}(\frac{mN}{m})$	$\gamma_1(\frac{mN}{m})$	$\gamma_2(\frac{mN}{m})$
36	0	0	5.32071	0.036383	5.06962207
38	0	0	4.87353	0.03642	5.36543752
40	0	0	4.611629	0.040864	5.81821494
36	1	0	3.969283	0.04712	5.37387081
38	1	0	3.84921	0.05353	5.27759774
40	1	0	3.681471	0.0425	5.43196499
36	1	0.5	2.58332	0.05108	4.87171008
38	1	0.5	2.482537	0.05786	5.50334844
40	1	0.5	2.328801	0.05027	5.72676155

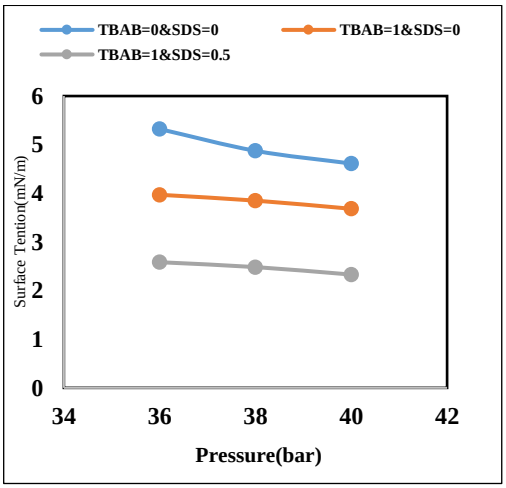

Figure 6. Effect of TBAB and SDS on interfacial tension of carbon dioxide hydrate at different pressures

Figure 6 shows that increasing pressure leads to a reduction in the interfacial tension of carbon dioxide. The addition of TBAB also leads to a decrease in interfacial tension and, as the TBAB concentration increases, interfacial tension decreases further.

As for Table 3, the interfacial tension values were given at different temperatures and concentrations of SDS at a constant pressure of 36 bar and in the presence of TBAB at a concentration of 1% by weight.

Table 3. The interfacial tension of CO_2 hydrate at 36 bar and different temperatures and SDS as estimated by applying experimental results into the CNT and values calculated using Eqs. (17) and (18)

T(K)	SDS(gr)	$\gamma_{exp}(\frac{mN}{m})$	$\gamma_1(\frac{mN}{m})$	$\gamma_2(\frac{mN}{m})$
274.15	0	3.920658	0.04526	4.83201057
276.15	0	3.969283	0.04712	5.37387081
278.15	0	4.100015	0.04822	5.98387769
274.15	0.5	2.421247	0.06163	5.3347903
276.15	0.5	2.58332	0.05108	4.87171008
278.15	0.5	2.688571	0.04838	3.65104104

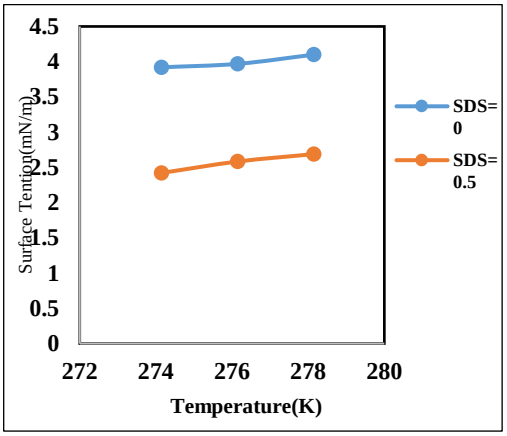

Figure 7. The effect of SDS on interfacial tension of CO_2 hydrate at different temperatures

In Figure 7, it is also observed that the increase in temperature increases interfacial tension and, in contrast to the addition of SDS to the system, it leads to a reduction in interfacial tension.

Table 4 shows that interfacial tension values for different temperatures and concentrations if TBAB at constant pressure of 26 bar.

Table 4. The interfacial tension of CO_2 hydrate at 36 bar and different temperatures and concentrations of TBAB as estimated by applying experimental results into the CNT and values calculated using Eqs. (17) and (18)

T(K)	P(bar)	TBAB (%wt)	$\gamma_{exp}(\frac{mN}{m})$	$\gamma_1(\frac{mN}{m})$	$\gamma_2(\frac{mN}{m})$
274.15	36	3	3.89397	0.04526	4.83201057
276.15	36	3	3.930668	0.047123	5.37387081
278.15	36	3	3.980253	0.048218	5.98383769
274.15	36	5	3.850796	0.047058	5.27135204
276.15	36	5	3.904707	0.051323	5.5979727
278.15	36	5	3.959313	0.049832	5.91771098

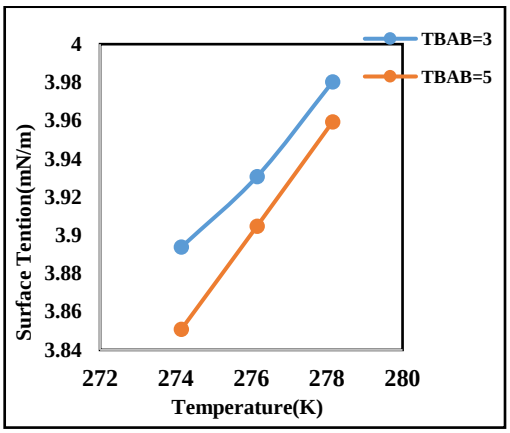

Figure 8. The effect of TBAB on interfacial tension of CO_2 hydrate at different temperatures

In Figure 8, the effect of TBAB on the interfacial tension of CO_2 hydrate is shown. As shown, the values of interfacial tension decrease with the addition of TBAB. On the other hand, increasing the temperature has the opposite effect and increases the amount of interfacial tension. In Table 5, interfacial tension values at different concentrations of TBAB and SDS are given at a constant temperature and pressure of 247.51 K and 36 bar.

Table 5. Interfacial tension of CO_2 hydrate at 247.5 K and 36 bar and different concentrations of TBAB and SDS as estimated by applying experimental results into the CNT and values calculated using Eqs. (17) and (18)

P(bar)	T(K)	TBAB (%wt)	SDS(gr)	$\gamma_{exp}(\frac{mN}{m})$	$\gamma_1(\frac{mN}{m})$	$\gamma_2(\frac{mN}{m})$
36	276.15	0	0	4.617728	0.036383	5.06962207
36	276.15	1	0	3.924302	0.047123	5.37387081
36	276.15	1	0.5	2.58332	0.051082	4.87171008

According to Tables 3, 4 and 5, it can be observed that the experimental values of the interfacial tension between the CO_2 hydrate and water obtained in this work are more consistent with Eq. 18.

This correlation can be due to the existence of the term $v_m^{-\frac{2}{3}}$ in both equations 10 and 18.

Determination of the order of nucleation:

According to equation 16, n is the order of nucleation which is calculated from the empirical data. By plotting $Ln\, t_{ind}$ versus $Ln\, S$ at different temperatures, n can be obtained from the slope of the line.

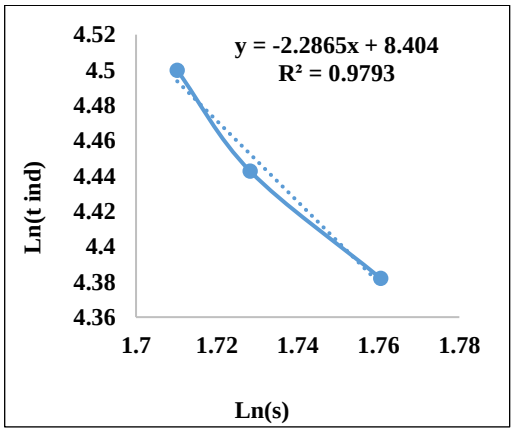

Figure 9. Nucleation order at 274.15 K and 38 bar

According to Figure 9, the order of nucleation (n) equals 2.2865 and the regression coefficient (R^2) is 0.9793.

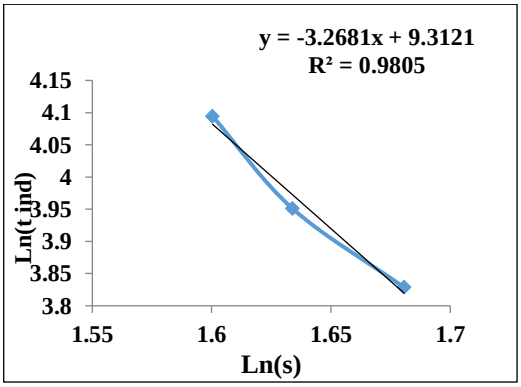

Figure 10. Nucleation order at 276.15 K and 38 bar

According to Figure 10, the order of nucleation (n) at 276.15 K and 38 bars is 3.2681 with a regression coefficient (R^2) of 0.9805 [35-37].

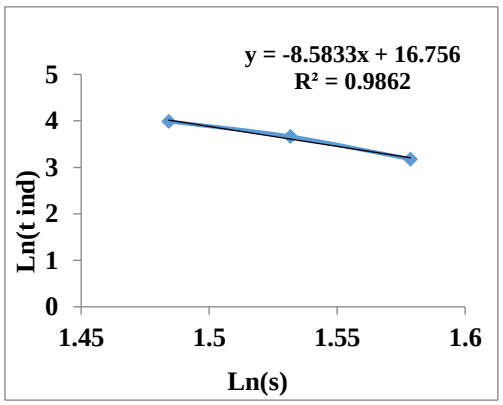

Figure 11. Nucleation order at 278.15 K and 38 bar

In Figure 11, the order of nucleation (n) is 8.5833 with a regression coefficient (R^2) of 0.9862.

Conclusion

In this study, interfacial tension, order of nucleation and super saturation were calculated at different temperatures, pressures, and concentrations of TBAB and SDS. The interfacial tension was calculated by measuring the induction time. According to the experimental results, the crystallization induction time decreased with increasing solution concentration at a constant temperature. In addition, the interfacial tension increased with increasing temperature, but it did not change with variations in the super saturation. The addition of SDS 500 ppm at the same pressure and concentration of TBAB decreased induction time and interfacial tension with increasing temperature. On the other hand, the induction time was still decreasing at the same temperature, but the interfacial tension did not change significantly. From the fitting of experimental data, the relationship between nucleation rates with super saturation was obtained. According to equations and graphs, the nucleation rate

is a function of temperature. Experimental data also showed a good agreement with the Classical Nucleation Theory [38-40].

Acknowledgement

This paper was extracted from a PhD thesis entitled "Theoretical and Experimental Study of CO_2 hydrate formation in the presence of surfactants and nanoparticles", conducted in the Department of Chemical Engineering, Mahshahr Branch, Islamic Azad University, Mahshahr, Iran.

References

[1] S. Li, S. Fan, J. Wang, X. Lang, Y. Wang, *Chin. J. Chem. Eng.*, **2010**, *18*, 202-206.
[2] E.D. Sloan, C.A. Koh, *third ed. CRC Press. Taylor and Francis Group, Boca Raton*, **2008**.
[3] J. Zheng, K. Bhatnagar, M. Khurana, P. Zhang, B.Y. Zhang, P. Lingaa, *Appl. Energy*, **2018**, *217*, 377–389.
[4] W. Lee, Y.S. Kim, S.P. Kang, *Chem. Eng. J.*, **2017**, *331*, 1-7.
[5] O. Antunes, Carollina de M. Molinari, N. Marcelino, A. Celina Kakitani, Moisés, R. Morales, E. M.S. Rigoberto, K. Amadeu, Braz. *J. Chem. Eng.*, **2018**, *35*, 265-274.
[6] M. Manteghian, S.M. Mousavi Safavi, A. Mohammadi, *Chem. Eng. J.*, **2012**, *2179*, 379-384.
[7] Z. Bohstrom, K.P. Lillerud, *J. Cryst. Growth*, **2018**, *498*, 154-159.
[8] A. Yamasaki, M. Wakatsuki, H. Teng, Y. Yanagisawa, K. Yamada, *Energy*, **1999**, *25*, 85-96.
[9] R. Larsen, C.A. Knight, E.D. Sloan, *Fluid Phase Equilibrium*, **1998**, *150*, 353–360.
[10] M.T. Mota-Martinez, S. Samdani, A.S. Berrouk, M.C. Kroon, C. J. Peters, *Ind. Eng. Chem. Res.*, **2014**, *53*, 20032–20035.
[11] N.S. Yuritsyn, A.S. Abyzov, V.M. Fokin, *J. Non-Cryst. Solids*, **2018**, *498*, 42–48.
[12] A.M. Rodrigues, D.R. Cassar, V.M. Fokin, E.D. Zanotto, *J. Non-Cryst. Solids*, **2017**, *479*, 55–61.
[13] J. Orava, A.L. Greer, *J. Non-Cryst. Solids*, **2016**, *451*, 94–100.
[14] A. Azimi, M. Mirzaei, *Chem. Eng. Res. Des.*, **2016**, *111*, 262-268.
[15] H. Mozaffar, R. Anderson, B. Tohidi, *Fluid Phase Equilibrium*, **2016**, *425*, 1-8.
[16] Z. Rezvani, K. Nejati, S. Alizade, S. Samuey, *J. Iran. Chem. Soc.*, **2016**, *4*, 347-358
[17] S. Babaee, H. Hashemi, A.H. Mohammadi, P. Naidoo, D. Ramjugernath, *J. Chem. Thermodyn.*, **2017**, *116*, 121–129.
[18] A. Azimi, M. Mirzaei, S.M. Tabatabaee Ghomshe, *Bulg. Chem. Commun.*, Special Issue D, **2015**, *47*, 49 – 55.
[19] A. Li, L. Jiang, S. Tang, *Energy*, **2017**, *134*, 629-637.
[20] M. Manteghian, A. Azimi, J. Towfighi, *J. Chem. Eng. Jpn.*, **2011**, *44*, *936-942*.
[21] J.W. Mullin, *Crystallization. Butterworth– Heinemann, Oxford*, **2001**.
[22] B.Y. Zhang, Q. Wu, D. Sun, *J. China Univ. Min. Technol.*, **2008**, *18*, 18-21.
[23] A. Rasoolzadeh, J. Javanmardi, A. Eslamimanesh, A.H. Mohammadi, *J. Mol. Liq.*, **2016**, *221*, 149–155.
[24] S. Ghader, M. Manteghian, M. Kokabi, R. Sarraf, *Chem. Eng. Technol.*, **2007**, *30*, 1-6.
[25] H. Luo, C.Y. Sun, Q. Huang, B. Z. Peng, G. J. Chen, *J. Colloid Interface Sci.*, **2005**, *297*, 266–270.
[26] K. Fukuzawa, K. Watanabe, K. Yasuda, R. Ohmura, *J. Chem. Thermodyn.*, **2017**, *119*, 20-25.
[27] H. Akiba, R. Ohmura, *J. Chem. Thermodyn.*, **2016**, *97*, 83-87.

[28] A. Mersmann, *J. Cryst. Growth*, **1994**, *147*, 181-193.
[29] P. Bennema, O. Sohnel, *J. Cryst. Growth*, **1990**, *102*, 547-556.
[30] E. Teymoori, A. Davoodnia, A. Khojastehnezhad, N. Hosseininasab, *Iran. Chem. Commun.* **2019**, *7*, 271-282
[31] A. Samimi., S. Zarinabadi, *Aust. J. Basic Appl. Sci.*, **2011**, *5*, 752-756
[32] A. Samimi., S. Zarinabadi, *Aust. J. Basic Appl. Sci.*, **2011**, *5*, 741-745
[33] A. Samimi., S. Zarinabadi, *J. Fundam. Appl. Sci.*, **2016**, *8*, 1160-1172
[34] S. Zarinabadi, A. Esfandiyari., S.A, Khodami., A. Samimi., *J. Fundam. Appl. Sci.*, **2016**, *8*, 1133-1149
[35] S. Janitabar Darzi., N. Mohseni., *Adv. J.Chem. A*, **2019**, *2*, 165-174
[36] A. Asweisi, R, Hussein, N, Bader, R, Elkailany, *Adv. J. Chem. A*, **2020**, *3*, In press.
[37] F. Ahmad, *Adv. J. Chem. A.*, **2020**, *3*, 70-93
[38] A, Samimi, S. Zarinabadi, A. Shahbazi Kootenaei, A. Azimi, M. Mirzaei, *J. Chem. Rev.*, **2019**, *1*, 164-182
[39] H. Hamidi, M.M. Heravi, M. Tajbakhsh, M. Shiri, H.A. Oskooie, S.A. Shintre, N.A. Koorbanally, *J. Iran. Chem. Soc*., **2015**, *12*, 2205-2212
[40] M.M. Heravi, K.H. Bakhtiari, M.H. Tehrani, N.M. Javadi, H.A. *Oskooie*, *Arkivoc*., **2006**, (xvi), 16-22.

How to cite this manuscript: Hamid Sarlak, Alireza Azimi, Seyed Mostafa Tabatabaee Ghomshe, Masoomeh Mirzaei. Effect of TBAB and SDS surfactants on the interfacial tension of CO_2 Hydrate in water. *Eurasian Chemical Communications*, 2020, 2(3), 319-328.